J Nanostruct 14(2): 599-607, Spring 2024

RESEARCH PAPER

Synthesis and Characterizations of Conductive Polymer-Metal Oxide Hybrid Nanocomposites Using V_2O_5, TiO_2 and Polypyrrole

Hamid Dehghan-Manshadi [1], *Mohammad Mazloum-Ardakani* [2*], *Sayed Ahmad Mozaffari* [1]

[1] *Thin Layer and Nanotechnology Laboratory, Department of Chemical Technologies, Iranian Research Organization for Science and Technology (IROST), Tehran, Iran*

[2] *Department of Chemistry, Faculty of Science, Yazd University, Yazd, Iran*

ARTICLE INFO

Article History:
Received 04 January 2024
Accepted 25 March 2024
Published 01 April 2024

Keywords:
Conductive polymers
Hybrid nanocomposites
Metal oxides
Photocatalytic activity
Ultrasound irradiation

ABSTRACT

Characterizations of conductive polymers can improve through their hybridization with other materials. In this work, an ultrasound-based method was employed to synthesize conductive polymer-metal oxide (CPMO) hybrid nanocomposites in the presence of pyrrole and different percentages of vanadium and titanium oxides. FESEM images indicated cubic-shape vanadium oxide and spherical-shape titanium oxide are distributed in polypyrrole matrix. Electrochemical impedance spectroscopy and direct measuring resistance were used to evaluate the electrical properties of the synthesized nanocomposites. The optimized CPMO hybrid nanocomposite (0.5 g vanadium oxide and 0.5 titanium oxide) displayed a relatively good electrical properties such as charge transfer resistance of 5.12 k Ω and resistance of 78.1 Ω.square^{-1}. Also, the synthesized CPMO hybrid nanocomposite showed a good photocatalytic activity through degradation of methylene blue with a degradation rate constant of 16.1×10^{-3} min^{-1} and efficiency of 87.3 % and 120 min. The synergetic effects of vanadium oxide and titanium oxide in the synthesized nanocomposites improved their functional features.

How to cite this article
Dehghan-Manshadia H., Mazloum-Ardakani M., Mozaffaria S. A. Synthesis and Characterizations of Conductive Polymer-Metal Oxide Hybrid Nanocomposites using V_2O_5, TiO_2 and Polypyrrole. J Nanostruct, 2024; 14(2):599-607. DOI: 10.22052/JNS.2024.02.021

INTRODUCTION

Conductive polymers have a wide applications in various fields such as electrical, sensors, energy devices, and optoelectronic due to their characterizations including easy fabrication, acceptable environmental stability, tunable electrical properties, and good optical and mechanical properties [1, 2]. They are important in preparaing various micro- and nano-structures with customized chemical and physical characterizations [3]. Polypyrrole (PPy) is an inherently conductive polymer with several advantages such as good electrical properties, high conductivity, biocompatibility, low cost and high stability. The broad π–electron conjugation of conjugated double bonds in the structure of conductive polymers is the reason for their good conductivity, which can improved via doping using protonation or reduction/oxidation reactions [4, 5]. One of the ways to increase the efficiency of polypyrrole is the polymerization of pyrrole in the presence of other compounds to synthesize a high performance nanocomposite. The structure of nanocomposite leads to a better dispersion of the individual components, maximization of their interactions and improvement of properties [6, 7].

* *Corresponding Author Email: mazloum@yazd.ac.ir*

Metal oxides have an important role in chemistry and material science because of their unique physical and chemical properties. In addition, their catalytic performance and physicochemical properties can be easily regulated according to the required characteristics. Metal oxide-based nanostructures have been widely used in various fields such as energy storage devices, catalysis, sensors, adsorbing pollutants and others [8-10]. Synthesis of a nanocomposite containing polypyrrole and metal oxides can result in unique properties and synergistic effects, combining the electrical conductivity of PPy with the specific properties of metal oxides. Several Researche studies have been reported on the application of metal oxides in modification of conductive polymers. Among them, vanadium and titanium oxides can be considered as a good candidate for enhancing properties of polypyrrole due to their good properties such as availability, high mechanical and thermal stability, high conductivity and low cost [5]. Polypyrrole is a conductive polymer, and the addition of vanadium and titanium oxides can enhance its electrical conductivity. These nanoparticles act as conductive fillers and facilitate the electron transport within the nanocomposite. On the other hand, The inclusion of vanadium and titanium oxides can improve the mechanical strength and stability of polypyrrole in the nanocomposite. Titanium oxide NPs are known for their excellent photocatalytic and optical properties, including high absorption in the UV region and good photoconductivity. It can enhanced photocatalytic and optical characterization of the prepared nanocomposite. Also, vanadium oxides NPs possess unique properties such as high redox activity and electrochemical performance [11-14]. Therefore, Adding these nanoparticles into polypyrrole can lead to synergistic effects, enabling applications in preparation of energy storage devices, catalysis, and sensors.

In this work, several CPMO hybrid nanocomposites were prepared using vanadium and titanium oxides as the metal oxides and polypyrrole as the conductive polymer through an ultrasound-based method. CPMO hybrid nanocomposites were fabricated using different percentages of vanadium and titanium oxides and their characterizations were investigated using FESEM, EDX, FTIR and XRD analysis. Also, electrical properties and photocatalytic activity of the synthesized CPMO hybrid nanocomposites were evaluated.

MATERIAL AND METHODS

Materials

Pyrrole (67.09 g/mol), titanium dioxide and vanadium pentoxide were purchased from Merck Co. and Iron (III) chloride hexahydrate and potassium chloride were received from Sigma Aldrich Co. All solutions were prepared using deionized water.

Synthesis of CPMO Hybrid Nanocomposites

TiO_2– V_2O_5–PPy nanocomposites were synthesized according to our previous work [5] with different percentages of components. In summary, various amounts of titanium dioxide (samples 1–5: 0.30, 0.40, 0.50, 0.60, 0.70 g) and vanadium pentoxide (samples 1–5: 0.70, 0.60, 0.50, 0.40, 0.30 g) were added to 10 mL aqueous solution of iron (III) chloride hexahydrate 0.10 mol L^{-1}. The prepared mixtures were sonicated using a SONICA 2200EP S3 ultrasonic bath device at 25 °C for 30 min. Then, 1 mL pyrrole 1 mol L^{-1} was added drop by drop to the obtained solutions. They were stirred with a magnetic stirrer in the presence of nitrogen gas with a flow rate of 20 mL min^{-1} at 8 °C for 2 h. Five CPMO hybrid nanocomposites were obtained according to Table 1.

Characterization of the Prepared CPMO Hybrid Nanocomposites

FESEM images and EDX patterns of the prepared CPMO hybrid nanocomposites were obtained

Table 1. Contents of the prepared CPMO hybrid nanocomposites

Samples	iron (III) chloride hexahydrate (mL)	Pyrrole (mL)	Titanium dioxide (g)	Vanadium pentoxide (g)
T3V7@PPy	10	1	0.30	0.70
T4V6@PPy	10	1	0.40	0.60
T5V5@PPy	10	1	0.50	0.50
T6V4@PPy	10	1	0.60	0.40
T7V3@PPy	10	1	0.70	0.30

by a Tescan, MIRA3 LM FESEM device coupled with EDX. FT-IR spectra of the prepared CPMO hybrid nanocomposites were recorded using a Bruker Equinox 55 single beam spectrometer in the wavenumber range from 4000 cm^{-1} to 400 cm^{-1}. Their XRD patterns were recorded using

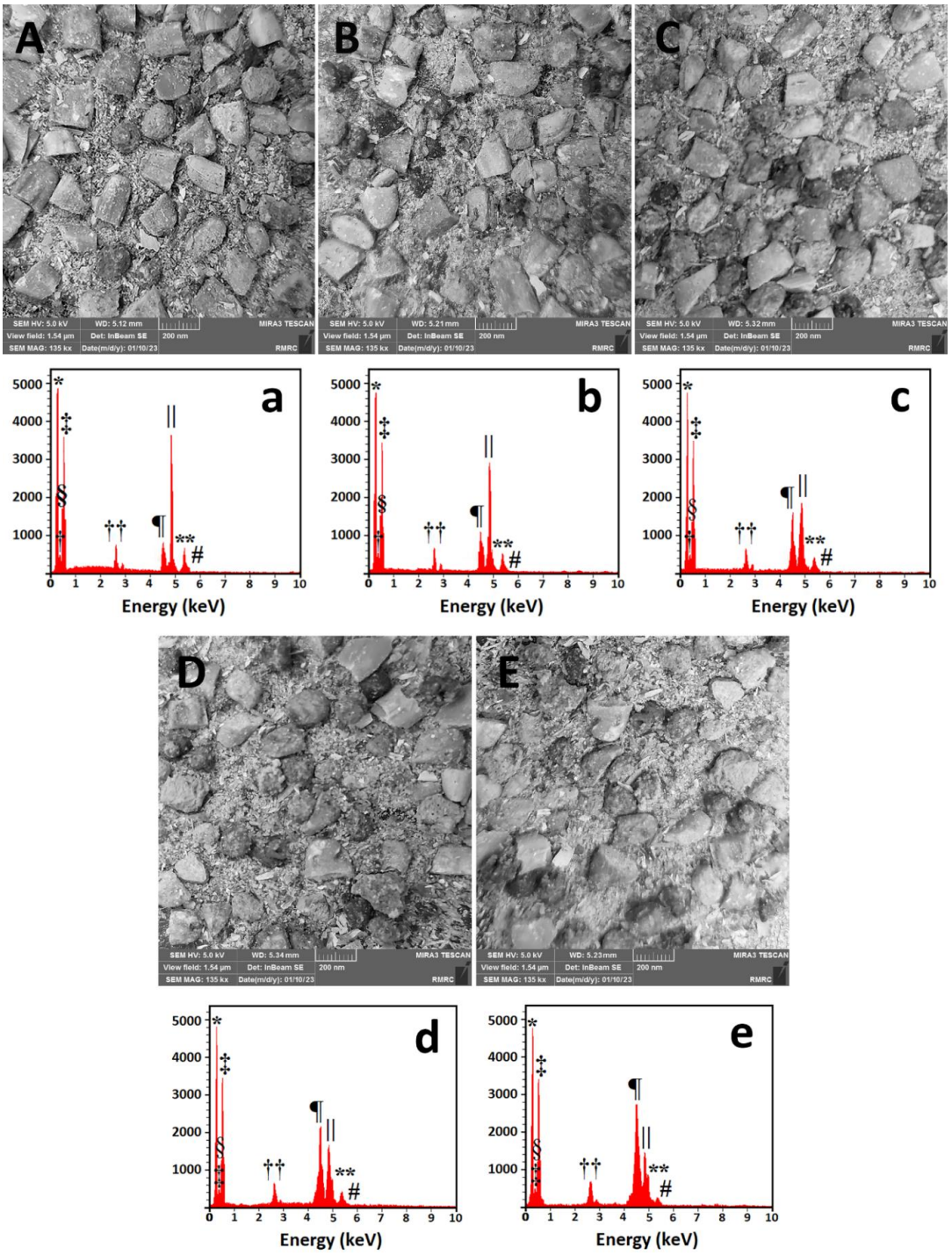

Fig. 1. FESEM images of A) T3V7, B) T4V6, C) T5V5, D) T6V4 and E) T7V3, and related EDX patterns. *CKα; † NKα; ‡ OKα; § VLα; ||VKα; #VKβ; ¶ TiKα; **TiKβ and ††Cl

an Asenware AW-DX300 diffractometer device equipped with Cu Kα radiation (λ = 1.54184 A°) in the 2θ range from 20° to 80°.

The electrical properties of the prepared CPMO hybrid nanocomposites were evaluated through two methods; 1) directly measuring their resistance using a digital multimeter (3200 Hioki HiTester), and 2) comparing their parameters using electrochemical impedance spectroscopy (EIS). EIS experiments were carried out using a Zive SP2 potentiostat/galvanostat connected to a three-electrode system including various CPMO hybrid nanocomposites as the working electrode, an Ag/AgCl electrode (Metrohm) as the reference electrode and a Pt electrode (Metrohm) as the counter electrode. A solution containing $Fe(CN)_6^{3-}$/ $Fe(CN)_6^{4-}$ 10 mmol.L^{-1} and KCl 0.1 mol.L^{-1} was used as the electrolyte. EIS data are recorded in the frequency range from 100 kHz to 0.100 Hz with an AC amplitude of 10 mVs^{-1}.

The photocatalytic activity of the synthesized CPMO hybrid nanocomposite was evaluated through study of photodegradation of methylene blue under UV irradiation using a 400 W Halogen lamp at a distance of 10 cm from the sample. The sample including 10 mg of the prepared CPMO hybrid nanocomposites was suspended into 50 mL methylene blue solution (10 ppm) and sonicated for 30 min. The suspension was stirred in dark for 30 min to achieve adsorption–desorption equilibrium of methylene blue. 2 mL of the mixture was centrifuged and the remaining methylene blue was analyzed using an Optizen 322 Double beam UV/Vis spectrophotometer at 666 nm. The solution was taken in dark for 20 min and transferred under the Halogen lamp to complete the procedures by analyzing their UV-Vis spectra at fixed intervals. The photocatalytic degradation efficiency and degradation rate constant (k) were calculated using the following equations:

$$\%\ \text{Degradation} = \frac{C_0 - C_t}{C_0} \quad (1)$$

$$\ln C_0 - \ln C_t = kt \quad (2)$$

$$\ln C_t = -kt + \ln C_0 \quad (3)$$

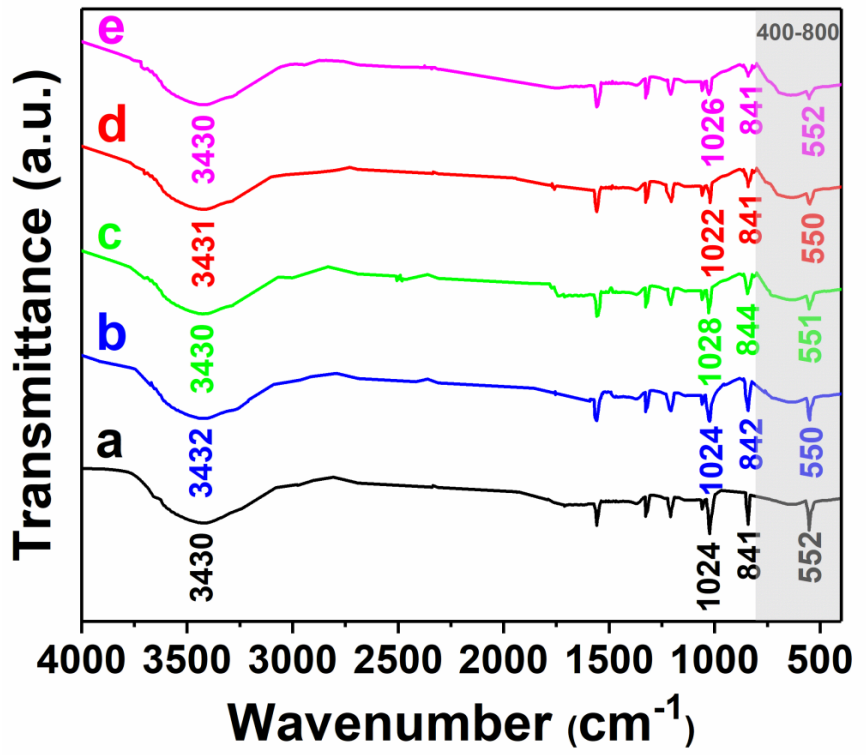

Fig. 2. FT-IR spectra of the synthesized nanocomposites with different amounts of titanium dioxide and vanadium pentoxide: a) T3V7, b) T4V6, c) T5V5, d) T6V4 and e) T7V3.

Where C_0 and C_t are the concentration of methylene blue before irradiation and after various irradiation times (t), respectively. Therefore, plotting ln C_t against time obtains a straight line graph with slope of –k and intercept of ln C_0 [15].

RESULTS AND DISCUSSION

FESEM and EDX

FESEM images and EDX patterns of the synthesized CPMO hybrid nanocomposites are indicated in Fig. 1. As seen, the cubic-shaped V_2O_5 nanoparticles and the spherical-shaped TiO_2 nanoparticles are well distributed in PPy matrix. Fig. 1A shows a large percentage of V7T3 CPMO hybrid nanocomposite including the cubic-shaped V_2O_5 nanoparticles and its lower percentage is the spherical-shaped TiO_2 nanoparticles. The number of cubic-shape nanoparticles decreases and the number of spherical-shape nanoparticles increases with increasing the percentage of titanium oxide from sample V7T3 to sample V3T7. EDX patterns of the samples (Fig. 1 a-e) confirm successful synthesis of various samples of CPMO hybrid nanocomposites. Comparing the EDX patterns of different CPMO hybrid nanocomposites shows that the intensity of the peaks related to vanadium oxide (§: VLα; ||: VKα and #: VKβ) is decreased with the decrease of its amount from sample V7T3 to sample V3T7. Conversely, the intensity of the peaks related to titanium oxide (¶: TiKα and **: TiKβ) is increased with the increase of its amount from sample V7T3 to sample V3T7.

FT-IR

The successful synthesis of various CPMO hybrid nanocomposites was evaluated by measuring their FT-IR spectra. Figs. 2a-e indicate the FT-IR spectra of the synthesized nanocomposites with different amounts of titanium dioxide and vanadium pentoxide. FT-IR spectrum of T3V7 sample (Fig. 2a) indicates a broad peak appeared at 3430 cm^{-1} related to stretching vibration of N-H bonds of PPy and two peaks appeared at 1558 and 1209 cm^{-1} attributed to C=C and C-N bonds in the structure of PPy. The peak observed at about 400–800 cm^{-1} is related to Ti–O–Ti bonds in TiO_2 structure. The existence of V2O5 in T3V7 sample is confirmed through observing a peak related to V=O bonds at 1024 cm^{-1} and two peaks related to V–O–V bonds at 841 and 552 cm^{-1}.

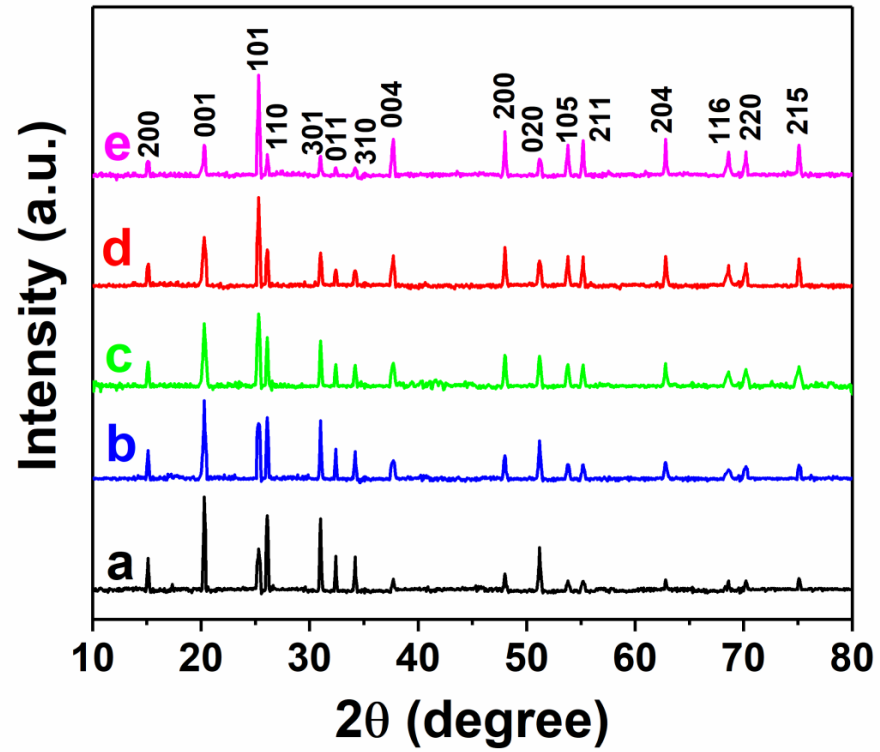

Fig. 3. XRD patterns of the synthesized nanocomposites with different amounts of titanium dioxide and vanadium pentoxide: a) T3V7, b) T4V6, c) T5V5, d) T6V4 and e) T7V3

FT-IR spectra of other samples show similar peaks with a little change in the height of the peaks which is related to percent of TiO_2 and V_2O_5 in their composition. For instance, the height of the broad peak at 400–800 cm^{-1} related to Ti–O–Ti bonds in T7V3 sample is increased compared to that of T3V7 sample due to increasing percent of TiO_2 component. Also, a decrease in the percent of V_2O_5 in T7V3 sample led to a reduction in the height of the peaks related to V=O and V–O–V bonds.

XRD

XRD patterns of the synthesized CPMO hybrid nanocomposites are indicated in Fig. 3. The appeared peaks at 2θ = 25.3°, 37.7°, 48°, 53.8°, 55.2°, 62.8°, 68.6°, 70.2°.and 75.1° related to (101), (004), (200), (105), (211), (204), (116), (220) and (215) reflections confirm the existence of TiO_2 NPs in the synthesized nanocomposites [16, 17]. Also, the existence of V_2O_5 NPs in the synthesized nanocomposites resulted in the appearance of the peaks at 2θ = 15.1°, 20.3°, 26.1°, 31°, 32.4°, 34.2° and 51.2° related to (200), (001), (110), (301), (011), (310) and (020) reflections, respectively [18, 19]. As seen, the peaks related to reflections of V_2O_5 NPs in T3V7 sample appeared with higher height against that of in T7V3 sample. Conversely, the peaks related to reflections of TiO_2 NPs have lower heights in T3V7 sample in comparison with T7V3 sample.

Electrical Properties

The electrical properties of various CPMO hybrid nanocomposites were investigated by extracting electrical parameters such as charge transfer resistance (R_{ct}) from EIS results as well as direct measuring of their resistance. EIS is a valuable technique that is widely applied in various research fields. This technique is based on applying a small perturbation of the potential or the current using an alternating small magnitude signal which leads to measuring impedance and phase shift data [20, 21]. For this purpose, EIS experiments were carried out using different CPMO hybrid nanocomposites. Fig. 4A displays the Nyquist plot of the synthesized CPMO hybrid nanocomposites in a solution containing $Fe(CN)_6^{3-}/Fe(CN)_6^{4-}$ 10 $mmol.L^{-1}$ and KCl 0.1 $mol.L^{-1}$. The Nyquist plots of samples V6T4 and V4T6 include a semicircle which represents the solution resistance at high frequencies and charge transfer resistance (diameter of semicircle in Z_{real} axis). In the Nyquist plots of samples V7T3, V5T5 and V3T7, a Warburg impedance is observed at low frequencies following the semicircle at high frequencies. This impedance expresses the difficulty of mass transport of the redox species to the electrode surface considering a semi-infinite linear diffusion [22]. A modified Randles equivalent circuit model was used as the equivalent circuit for fitting the EIS data. The curve of R_{ct} changes using various CPMO hybrid nanocomposites is displayed in Fig. 4B (red curve). According to obtained data, Sample V5T5 indicated a low value of charge transfer resistance (5.12 kΩ) compared to other CPMO hybrid nanocomposites. Samples V7T3 with R_{ct} = 27.1 kΩ and V3T7 with R_{ct} = 31.8 kΩ have low conductivity against other samples.

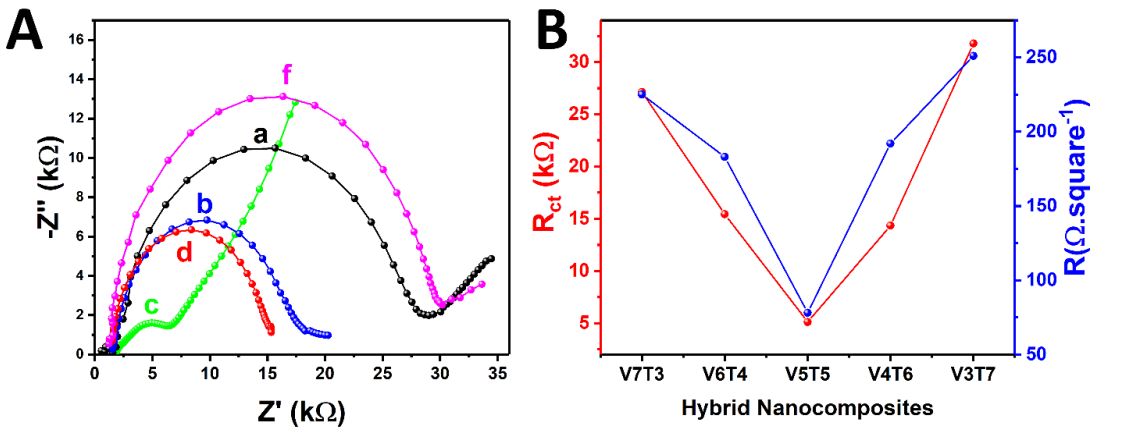

Fig. 4. A) The nyquist plots of the syntheized hybrid nanocomposites in a solution containing $Fe(CN)_6^{3-}/Fe(CN)_6^{4-}$ 10 $mmol.L^{-1}$ and KCl 0.1 $mol.L^{-1}$: a) T3V7, b) T4V6, c) T5V5, d) T6V4 and e) T7V3; B) The curves of Rct changes extracted from nyquist plots (red curve) and resistance changes (blue curve) for various hybrid nanocomposites

The changes of resistance (direct measuring) for different nanocomposites are indicated in Fig. 4B (blue curve). As predicted based on the EIS results, the lowest value of resistance was 78.1 $\Omega.square^{-1}$ related to V5T5 nanocomposite. The resistance decreases with decreasing amounts of vanadium oxide in the structure of the synthesized nanocomposites from V7T3 sample to V5T3 sample. The value of resistance increases with increasing the percentage of titanium oxide in the content of nanocomposites from V5T5 sample to V7T3 sample.

According to the obtained results, the sample V5T5 indicated a relatively good conductivity. The shape of Nyquist plot related to sample V5T5 is distinct from other CPMO hybrid nanocomposites. As seen, at a low frequency, the imaginary part of the impedance is sharply increased indicating the capacitive behavior of this hybrid nanocomposite. Therefore, it can be utilized as the substrate in the design and fabrication of energy storage devices such as supercapacitors, solar cells and batteries. Modification of its surface using a suitable material can improve its properties such as conductivity and photocatalytic activity.

Photocatalytic Activity

Semiconductor materials can provide photo-generated holes with high oxidizing power due to their wide band gap energy. Photocatalytic activity of the nanocomposites prepared using titanium oxide and vanadium oxide was evaluated through a study of the degradation efficiency of methylene blue under exposure to UV-visible light. Sample V5T5 as the optimum CPMO hybrid nanocomposite was selected as the sample for

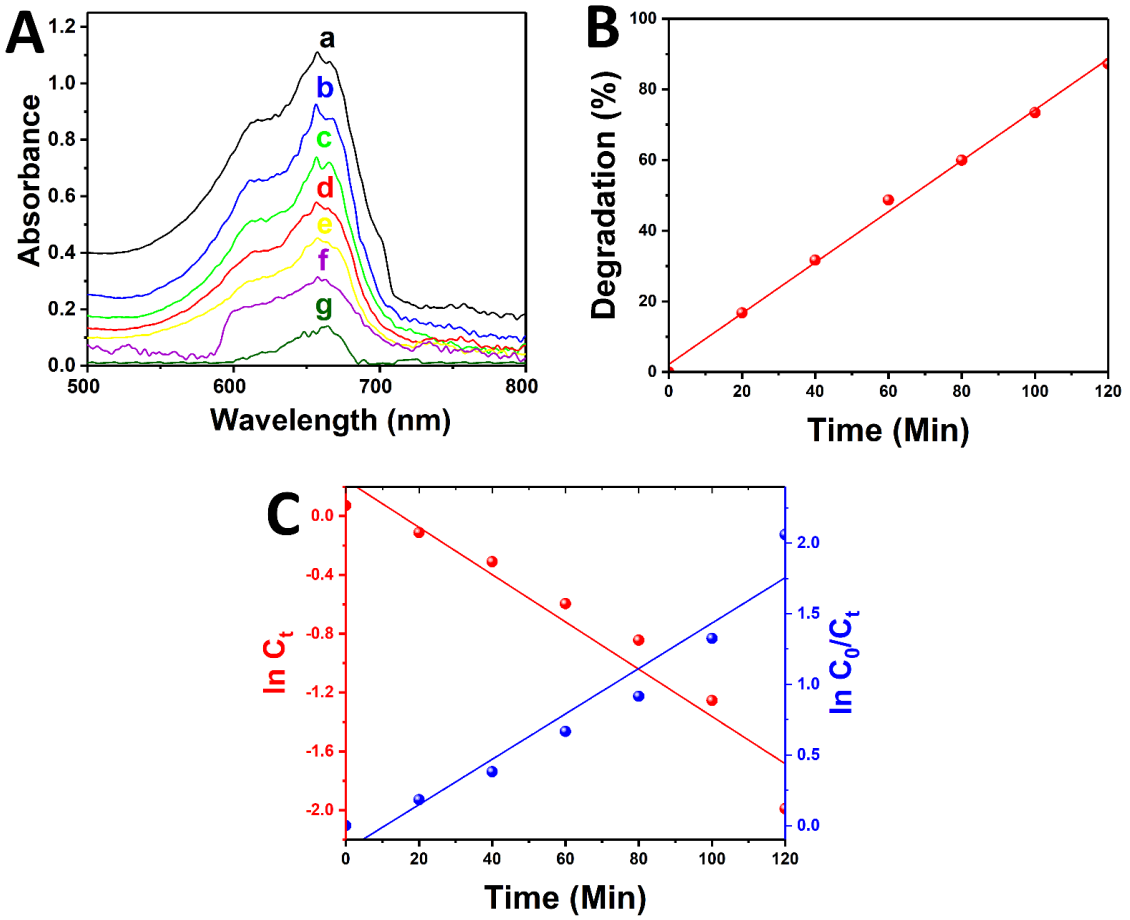

Fig. 5. A) UV–visible absorbance spectra of methylene blue photodegradation in presence of the synthesized hybrid nanocomposite after UV irradiation in different times of a) 0, b) 20, c) 40, d) 60, e) 80, f) 100 and g) 120 min; B) Degradation efficiency of methylene blue by hybrid nanocomposite; C) The curves of ln Ct (red curve) and ln Ct/C0 (blue curve) in in different UV irradiation times

$$TiO_2 + h\upsilon \rightarrow TiO_2(e^-_{CB} + h^+_{VB}) \quad (4)$$

$$V_2O_5 + h\upsilon \rightarrow V_2O_5(e^-_{CB} + h^+_{VB}) \quad (5)$$

$$TiO_2(e^-_{CB}) + V_2O_5(e^-_{CB}) + 2O_2 \rightarrow 2O_2^{\cdot -} + TiO_2 + V_2O_5 \quad (6)$$

$$TiO_2(h^+_{VB}) + V_2O_5(h^+_{VB}) + 2H_2O \rightarrow 2OH^{\cdot} + 2H^+ + TiO_2 + V_2O_5 \quad (7)$$

$$O_2^{\cdot -} + 2H^+ \rightarrow 2OH^{\cdot} \quad (8)$$

$$TiO_2(h^+_{VB}) + V_2O_5(h^+_{VB}) + O_2^{\cdot -} + OH^{\cdot} + \text{Methylene Blue} \quad (9)$$

$$\text{Methylene Blue}^{\cdot +} \rightarrow \text{Degradation} \quad (10)$$

investigation of photocatalytic activity. Fig. 5A indicates the absorbance spectra of methylene blue photodegradation in the presence of synthesized CPMO hybrid nanocomposite. As seen, the intensity of the absorbance peaks decreases with increasing time of exposure to UV-visible light. The photocatalytic degradation efficiency of methylene blue was investigated by extracting absorbance peak intensity of methylene blue at λ = 666 nm after UV irradiation in different times and in comparison with the initial absorbance. Fig. 5B displays the photocatalytic degradation of methylene blue using CPMO hybrid nanocomposite. The results indicated the photocatalytic degradation of methylene blue in the presence of CPMO hybrid nanocomposite reached to 87.3 % after 120 min. The curves of ln C_t versus time (red curve) and ln C_0/C_t versus time (blue curve) in Fig. 5C indicate a degradation rate constant of 16.1×10^{-3} min^{-1} for photocatalytic degradation of methylene blue using CPMO hybrid nanocomposite. The relatively good photocatalytic performance of the CPMO hybrid nanocomposite can be attributed to high band gap energy of titanium oxide and vanadium oxide and their ability to strong absorption of UV irradiation.

The proposed mechanism of photodegradation of methylene blue in the presence of CPMO hybrid nanocomposite is indicated in Eqs. 4-10.

The photocatalytic degradation of methylene blue is initiated by the formation of electron-hole pairs on the surface of the catalyst. Excitation of TiO_2 and V_2O_5 contents of the CPMO hybrid nanocomposites by the irradiation of UV light leads to absorption of energy by the electrons in the valence bands (VB) of vanadium and titanium oxides, jumping to the conduction bands (CB), and creating the holes in the valence band. Interaction of the obtained holes in the valance band with H_2O or OH^- leads to obtaining hydroxyl radicals ($OH^{\bullet}$) and interaction of $OH^{\bullet}$ and $O_2^{\bullet -}$ in the presence of h^+ results in photodegradation of methylene blue [23-25]. It seems that the mutual synergic effect of vanadium and titanium oxides enhances photocatalytic activity of the prepared CPMO hybrid nanocomposites.

CONCLUSION

The aim of this work is the fabrication of a high-performance CPMO hybrid nanocomposite using polypyrrole and metal oxides. Vanadium and titanium oxide were added in the polymerization procedure of pyrrole to enhance its characterizations. Several CPMO hybrid nanocomposites were synthesized using various percentages of vanadium and titanium oxides. Successful preparation of CPMO hybrid nanocomposites was confirmed using FESEM images, EDX, FTIR, and XRD analysis indicating a polypyrrole matrix containing distributed cubic-shape vanadium oxide and spherical-shape titanium oxide. Relatively good electrical properties (R_{ct} = 5.12 k Ω and R = 78.1 Ω·$square^{-1}$) and a good photocatalytic activity with a degradation rate

constant of 16.1×10^{-3} min^{-1} and efficiency of 87.3 % and after 120 min were the important results of the present work. Also, the synthesized CPMO hybrid nanocomposite showed. The synergetic effects of vanadium oxide and titanium oxide in the synthesized nanocomposites improved their functional features. The prepared CPMO hybrid nanocomposites can be selected as the substrate in preparation of optical sensors, electrochemical sensors, and energy storage devices such as supercapacitors, solar cells, and batteries.

ACKNOWLEDGEMENTS

The authors wish to thank the Research Council of Yazd University and Iranian Research Organization for Science and Technology (IROST) for financial support of this research.

CONFLICT OF INTEREST

The authors declare that there is no conflict of interests regarding the publication of this manuscript.

REFERENCES

1. K N, Rout CS. Conducting polymers: a comprehensive review on recent advances in synthesis, properties and applications. RSC Advances. 2021;11(10):5659-5697.
2. Tajik S, Beitollahi H, Nejad FG, Shoaie IS, Khalilzadeh MA, Asl MS, et al. Recent developments in conducting polymers: applications for electrochemistry. RSC Advances. 2020;10(62):37834-37856.
3. Idumah CI. Novel trends in conductive polymeric nanocomposites, and bionanocomposites. Synth Met. 2021;273:116674.
4. Borges MHR, Nagay BE, Costa RC, Souza JGS, Mathew MT, Barão VAR. Recent advances of polypyrrole conducting polymer film for biomedical application: Toward a viable platform for cell-microbial interactions. Advances in Colloid and Interface Science. 2023;314:102860.
5. Dehghan-Manshadi H, Mazloum-Ardakani M, Mozaffari SA. A flexible capacity-metric creatinine sensor based on polygon-shape polyvinylpyrrolidone/CuO and Fe2O3 NRDs electrodeposited on three-dimensional TiO_2–V_2O_5–Polypyrrole nanocomposite. Biosensors and Bioelectronics. 2024;246:115881.
6. Hao L, Yu D. Progress of conductive polypyrrole nanocomposites. Synth Met. 2022;290:117138.
7. Singh N. Polypyrrole-based emerging and futuristic hybrid nanocomposites. Polym Bull. 2021;79(9):6929-7007.
8. Danish MSS, Estrella LL, Alemaida IMA, Lisin A, Moiseev N, Ahmadi M, et al. Photocatalytic Applications of Metal Oxides for Sustainable Environmental Remediation. Metals. 2021;11(1):80.
9. Liu Q, Zhang A, Wang R, Zhang Q, Cui D. A Review on Metal- and Metal Oxide-Based Nanozymes: Properties, Mechanisms, and Applications. Nano-Micro Letters. 2021;13(1).
10. Goria K, Bharti A, Raina S, Kothari R, Tyagi VV, Singh HM, et al. Low-cost adsorbent biomaterials for the remediation of inorganic and organic pollutants from industrial wastewater: Eco-friendly approach. Sustainable Materials for Sensing and Remediation of Noxious Pollutants: Elsevier; 2022. p. 87-112.
11. Roy S, Mishra S, Yogi P, Saxena SK, Mishra V, Sagdeo PR, et al. Polypyrrole–vanadium oxide nanocomposite: polymer dominates crystallanity and oxide dominates conductivity. Appl Phys A. 2017;124(1).
12. Al-hakimi AN, Alminderej F, Alhagri IA, Al-Hazmy SM, Farea MO, Abdallah EM. Inorganic nanofillers TiO_2 nanoparticles reinforced host polymer polypyrrole for microelectronic devices and high-density energy storage systems. Journal of Materials Science: Materials in Electronics. 2023;34(3).
13. Zhou X, Chen X, He T, Bi Q, Sun L, Liu Z. Fabrication of polypyrrole/vanadium oxide nanotube composite with enhanced electrochemical performance as cathode in rechargeable batteries. Appl Surf Sci. 2017;405:146-151.
14. Yuan X, Kobylanski MP, Cui Z, Li J, Beaunier P, Dragoe D, et al. Highly active composite TiO_2-polypyrrole nanostructures for water and air depollution under visible light irradiation. Journal of Environmental Chemical Engineering. 2020;8(5):104178.
15. Karuppasamy P, Ramzan Nilofar Nisha N, Pugazhendhi A, Kandasamy S, Pitchaimuthu S. An investigation of transition metal doped TiO_2 photocatalysts for the enhanced photocatalytic decoloration of methylene blue dye under visible light irradiation. Journal of Environmental Chemical Engineering. 2021;9(4):105254.
16. Deivanayaki S, Ponnuswamy V, Mariappan R, Jayamurugan P. Synthesis and characterization of polypyrrole/TiO_2 composites by chemical oxidative method. Optik. 2013;124(12):1089-1091.
17. Chen J, Shu C, Wang N, Feng J, Ma H, Yan W. Adsorbent synthesis of polypyrrole/TiO_2 for effective fluoride removal from aqueous solution for drinking water purification: Adsorbent characterization and adsorption mechanism. Journal of Colloid and Interface Science. 2017;495:44-52.
18. Malook K, Khan H, Shah M, Ihsan Ul H. Synthesis, characterization and electrical properties of polypyrrole/V_2O_5 composites. Korean J Chem Eng. 2017;35(1):12-19.
19. Khan H, Malook K, Shah M. Highly selective and sensitive ammonia sensor using polypyrrole/ V_2O_5 composites. Journal of Materials Science: Materials in Electronics. 2017;28(18):13873-13879.
20. Electrochemical impedance spectroscopy. Nature Reviews Methods Primers. 2021;1(1).
21. Mazloum-Ardakani M, Manshadi AD, Bagherzadeh M, Kargar H. Impedimetric and Potentiometric Investigation of a Sulfate Anion-Selective Electrode: Experiment and Simulation. Anal Chem. 2012;84(6):2614-2621.
22. Lazanas AC, Prodromidis MI. Electrochemical Impedance Spectroscopy–A Tutorial. ACS Measurement Science Au. 2023;3(3):162-193.
23. El-Yazeed WSA, Ahmed AI. Photocatalytic activity of mesoporous WO_3/TiO_2 nanocomposites for the photodegradation of methylene blue. Inorg Chem Commun. 2019;105:102-111.
24. Mishra A, Panigrahi A, Mal P, Penta S, Padmaja G, Bera G, et al. Rapid photodegradation of methylene blue dye by rGO-V_2O_5 nano composite. J Alloys Compd. 2020;842:155746.
25. Sharma D, Faraz M, Kumar D, Takhar D, Birajdar B, Khare N. Visible light activated V_2O_5/rGO nanocomposite for enhanced photodegradation of methylene blue dye and photoelectrochemical water splitting. Inorg Chem Commun. 2022;142:109657.